Available online at www.sciencedirect.com
ScienceDirect
Sensors and Actuators A 141 (2008) 422–431
SENSORS AND ACTUATORS A PHYSICAL
www.elsevier.com/locate/sna

Hot embossing of micro-lens array on bulk metallic glass

C.T. Pan [a,*], T.T. Wu [a], M.F. Chen [a], Y.C. Chang [b], C.J. Lee [b], J.C. Huang [b]

[a] *Department of Mechanical and Electro-Mechanical Engineering, and Center for Nanoscience & Nanotechnology, National Sun Yat-Sen University, Kaoshiung 804, Taiwan, ROC*
[b] *Institute of Materials Science & Engineering, Center for Nanoscience and Nanotechnology, National Sun Yat-Sen University, Kaohsiung 804, Taiwan, ROC*

Received 5 April 2007; received in revised form 25 September 2007; accepted 14 October 2007
Available online 23 October 2007

Abstract

This study presents a new process to fabricate micro-lens array. The process of Micro-Electro-Mechanical Systems (MEMS) includes photoresist reflow technique, and nickel–cobalt (Ni–Co) electroplating to fabricate a first mold. Then, this first mold is applied to hot emboss on Mg–Cu–Y amorphous alloy to form a secondary mold. The secondary mold is a bulk metallic glass (BMG) material, whose thermal properties such as the glass transition temperature (T_g), the onset temperature for viscous flow (T_{onset}), the steady-state viscous flow temperature (T_{vs}), and the finish temperature for the viscous flow (T_{finish}) are investigated using differential scanning calorimetry (DSC) and thermomechanical analyzer (TMA). The glass transition temperature of BMG is around 140 °C (413 K). Therefore, the temperature of the hot embossing experiment is set at 423 K. This hot embossing process on BMG material makes molding process faster and more diverse applications. Next, the secondary mold is used to emboss on polymethylmethacrylate (PMMA) sheets. BMG is not only a good material for hot embossing process to fabricate micro-structure directly, but also fast-molding material for hot embossing process. Molding process using BMG material as a secondary mold can be more cost-effective and time-saving than the traditional MEMS process does.

Keywords: Molding; TMA; Amorphous; Secondary mold; Bulk metallic glass; DSC

1. Introduction

Bulk metallic glass (BMG) is referred to an amorphous metallic alloy that can be formed into bulk specimens with a minimum diameter greater than 1 mm. The materials show very high strength at room temperature and excellent viscous flow property at temperatures between the glass transition temperature (T_g) and crystallization temperature (T_x). In recent years, micro-lens array has been attracting much attention for a variety of applications. For display field, it is used to enhance the brightness of illumination and simplify the light guide module construction. Both higher accuracy and lower cost of micro-lens fabrication methods are needed to meet the rapid growth of the commercial devices. It is an important issue to make a high accuracy and strength mold to replicate micro-lens array precisely. The selection of BMG is based on the fact that amorphous alloys contain no dislocation that can be responsible for yielding in crystalline materials, and are therefore expected to be strong and hard.

The viscous flow behavior of the $Mg_{58}Cu_{31}Y_{11}$ bulk amorphous rods in the supercooled viscous region was investigated. It was found that the appropriate working temperature for micro-forming was about 460–474 K [1]. The maximum diameter of glass formation (D_c), T_g, temperature interval of the supercooled liquid region (ΔT_x), melting temperature (T_m), liquidus temperature (T_l) as well as heats of crystallization (ΔH_x) and melting (ΔH_m) were reported for Ga-based [2] and Mg-based bulk amorphous alloys [3]. Glass transition and crystallization behavior of several Mg–Ni–Nd metallic glasses have been systematically studied by temperature-modulated differential scanning calorimetry (TMDSC). It provided clear observation of glass transition and crystallization micro-mechanism [4]. The application of melt-spinning process of $Mg_{85}Cu_5Zn_5Y_5$ alloy was studied, which was found to cause the formation of a mixed structure consisting of nanoscale crystalline particles embedded in an amorphous matrix [5]. Yuan and Inoue reported that an

* Corresponding author. Tel.: +886 7 5252000x4239; fax: +886 7 254299.
E-mail address: panct@mail.nsysu.edu.tw (C.T. Pan).

0924-4247/$ – see front matter © 2007 Elsevier B.V. All rights reserved.
doi:10.1016/j.sna.2007.10.040

appropriate substitution of Cu by Ni in $Mg_{65}Cu_{25}Gd_{10}$ significantly improved its mechanical properties, especially improved the ductility of Mg-based bulk metallic glass [6]. It is known that BMG alloys can exhibit not only the unique physical properties such as excellent elasticity and strength, but also the significant plasticity occurred in the ΔT_x, due to a drastic drop in viscosity during glass transition upon heating [7]. Several researchers have reported the mechanical properties by uniaxial tensile testing [5,8,9] and uniaxial compression testing [1,3,6,10,11]. The literature indicated that BMGs exhibited high strength and brittle property at room temperature, and they also showed low stress and superplasticity at the supercooled liquid region. Mg–Cu–Y-based system exhibited reasonably good forming ability (GFA) with a wide supercooled liquid region before crystallization [12]. There have been numerous studies on the fabrication of BMGs. These literatures reported the forming ability of BMGs. Several kinds of BMGs were welded to BMGs or crystalline metals by liquid-phase welding using explosion, pulse-current and electron-beam methods, and by supercooled liquid-phase welding using friction method [13–16]. Turning [17] and drilling [18] were also tested and characterized.

However, there were only few studies on imprinting or hot embossing process of BMG material. Saotome et al. [19] used imprint process to fabricate nano-patterns. A silicon-based die was fabricated. With that die, they examined the nano-forming ability of Pd-based amorphous alloy. Chu et al. [20] reported the fabrication of a silicon-based grating die to imprint on $Pd_{40}Ni_{40}P_{20}$ plate, and then it was replicated on polymer.

The objective of this study is to fabricate a gapless hexagonal micro-lens array with high fill factor by this new embossing process. The previous study has reported fabrication of a Ni–Co mold of gapless hexagonal micro-lens array using LIGA-like process (LIGA, a German acronym for Lithographie, Galvanoformung, and Abformung) [21]. In this study, a modified molding process using $Mg_{58}Cu_{31}Y_{11}$ BMG as a secondary mold to replicate the gapless hexagonal micro-lens array is attempted. The schematic illustration is shown in Fig. 1. Before hot embossing process, the thermo-mechanical properties of the Mg-based

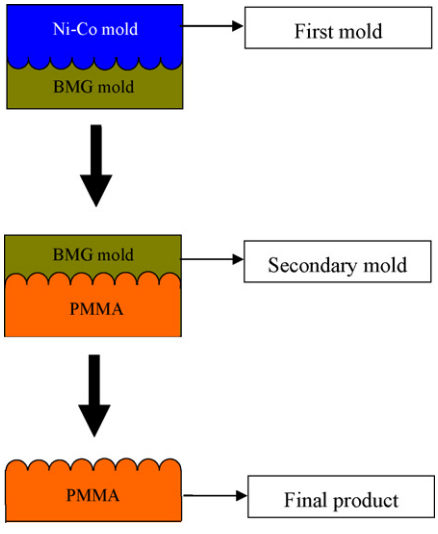

Fig. 1. The schematic replication process on the PMMA.

$Mg_{58}Cu_{31}Y_{11}$ system are investigated using differential scanning calorimetry (DSC) and thermomechanical analyzer (TMA). The working temperature for superplastic microforming is the one close to the glass temperature around 413 K. It shows experimentally that the optimum working temperature is dependent on the applied stress level. Since the BMG material has superplastic property at the supercooled liquid region, it can be easily formed by the master die. After cooling, the material has very high mechanical strength to be a secondary mold. Then, the BMG mold is used to replicate micro-lens array on the polymethylmethacrylate (PMMA) sheet. The embossing feasibility and degree of forming ability of the Ni–Co (first mold), BMG (secondary mold), and PMMA replica are compared and discussed.

2. Material

The $Mg_{58}Cu_{31}Y_{11}$ BMGs in the rod form with a diameter of 4 mm were prepared by a copper mold injection casting technique, through the induction melting of pure Mg and prealloyed Cu–Y ingots in an argon atmosphere. The basic thermal properties were first measured in a continuous heating mode by DSC (TA Instruments DSC 2920) and TMA (Perkin-Elmer Diamond). The applied heating rate was 10 K/min. The T_g, T_x and T_m are 413 K (140°C), 479 K (206 °C), and 711 K (438 °C), respectively, which are obtained by DSC.

Fig. 2(a) shows the temperature dependence of the relative displacement of the bulk amorphous $Mg_{58}Cu_{31}Y_{11}$ alloys obtained by TMA operated in the compression mode at various stress levels and a fixed heating rate of 10 K/min [1]. The maximum displacement (ΔL_{max}) occurred in the supercooled liquid region reaches 60.9, 162.6, 265.3, 748.8, and 923.3 μm under the applied compressive load of 0.8, 2.4, 7.1, 117.8, 318.5 kPa, respectively. Such displacements correspond to engineering strains $\Delta L_{max}/L_0$ (where L_0 is the original specimen height 4 mm) of 1.52%, 4.07%, 6.63%, 18.72%, and 23.08%. The relative displacements become pronounced at temperatures greater than T_g, indicating the high deformability of the glassy alloy in the ΔT_x.

Fig. 2(b) shows the typical TMA and differential thermomechanical analyzer (DTMA) curves measured at a stress level of 7.1 kPa on the bulk amorphous $Mg_{58}Cu_{31}Y_{11}$ alloys [1]. The DTMA curve is obtained from the derivative of the displacement with respect to time. The onset temperature for the viscous flow (T_{onset}), the semi-steady-state viscous flow temperature (T_{vs}), and the finish temperature for the viscous flow (T_{finish}), is marked on the TMA or DTMA curve. Thus, under a higher loading stress, crystallization tends to start at a lower temperature, and brings viscous flow to the end sooner.

3. Process procedures

The new process is used to fabricate a BMG mold to replicate micro-lens array on PMMA sheets. Two different molds are prepared, which are the first mold (Ni–Co) and the secondary mold ($Mg_{58}Cu_{31}Y_{11}$ BMG), respectively. The Ni–Co mold is used to replicate a secondary mold of Mg–Cu–Y amorphous alloy. Next, the secondary mold is applied to hot emboss on PMMA sheets.

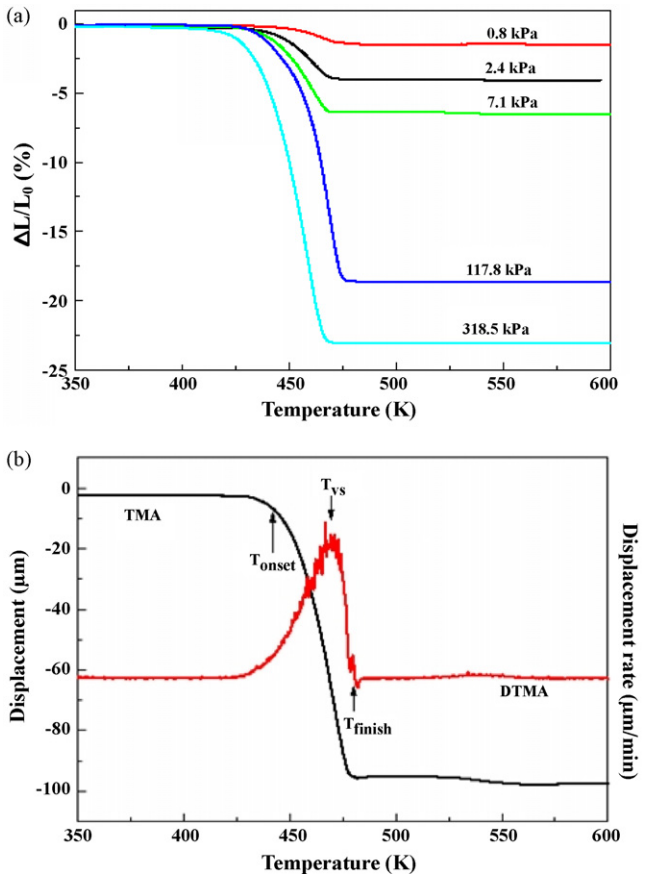

Fig. 2. Results of (a) temperature dependence of relative displacement and (b) typical TMA and DTMA curves measured at stress level of 7.1 kPa from the DSC and TMA for $Mg_{58}Cu_{31}Y_{11}$ [1].

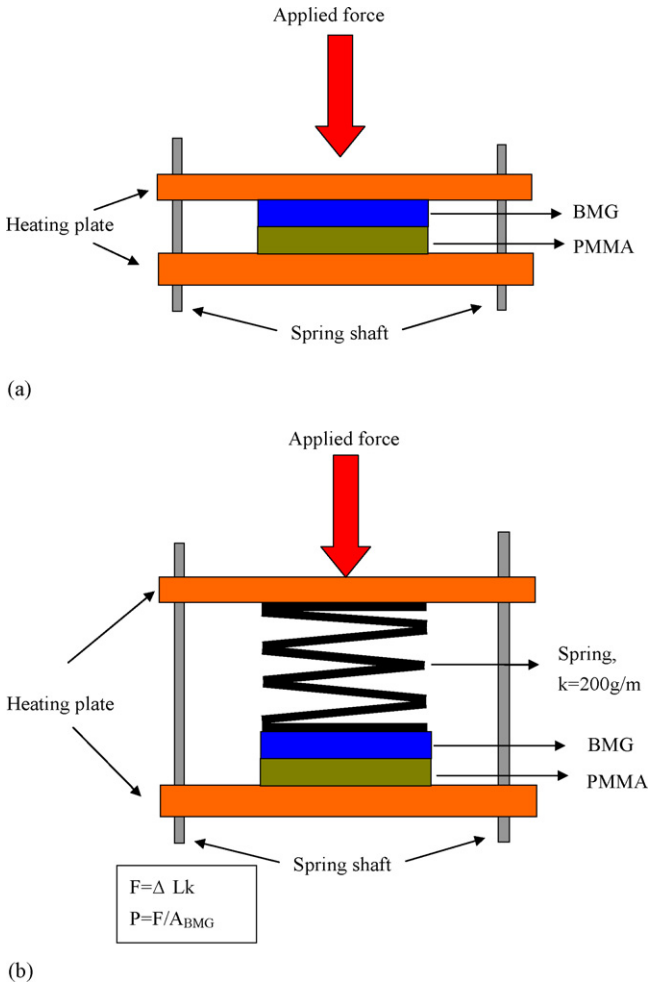

Fig. 3. Hot embossing set-up: (a) oil hydraulic system; (b) spring plate system.

3.1. First mold process

Four inch silicon wafer substrate was prepared for lithography process including the wafer cleaning process and dehydration baking etc.; first, the wafer was sent to prime the hexamethyldisilazane (HDMS) and spin coated with photoresist AZ4620. The spin rate was set at 1100 rpm for 25 s. The final thickness of 25 μm was obtained. Then, the silicon substrate was sent to the mask aligner to expose for 40 s after soft-baking at 85 °C. The dose of the exposure was 380 mJ. After developing, a column array on the silicon substrate was defined. And then, this structure was heated to a temperature above the photoresist glass temperature. The photoresist columns were melted and changed the photoresist profile into a hemispherical micro-lens array. After the hemispherical micro-lens array was completed, Ni thin film was sputtered on the hemispherical structure surface, served as seed layer. Then Ni–Co electroplating technique was used to form a hexagonal micro-lens mold, served as the first mold.

3.2. Secondary mold replicating process

The first mold was used to transfer the hexagonal micro-lens on the $Mg_{58}Cu_{31}Y_{11}$ alloy, served as the secondary mold. Two different hot embossing facilities including high and low pressure systems are set up for the embossing experiments, respectively. An oil hydraulic plate for the high pressure embossing system is shown schematically in Fig. 3(a). On the other hand, a spring plate for the low pressure system is illustrated schematically in Fig. 3(b). The oil hydraulic plate system provides large embossing pressure up to 2 MPa for the hot embossing process. And the spring plate provides much lower range of pressure (about several kPa) than that of the oil hydraulic plate. The reason is that BMG only requires much lower pressure level for embossing process than that required of PMMA. The deformability at different pressure levels is explored.

After the micro-lens patterns were transferred, the patterns on the first mold, the secondary mold and replica on PMMA were compared, respectively.

4. Results and discussions

In this study, a large dimension of gapless hexagonal micro-lens array of 330 μm in diameter of an inscribed circle is designed and fabricated. The experimental result of the Ni–Co mold is shown in Fig. 4. The dimension of the Ni–Co mold with gapless hexagonal micro-lens array is 3 cm × 3 cm in area. The reason why it is designed at such a large dimension is that the

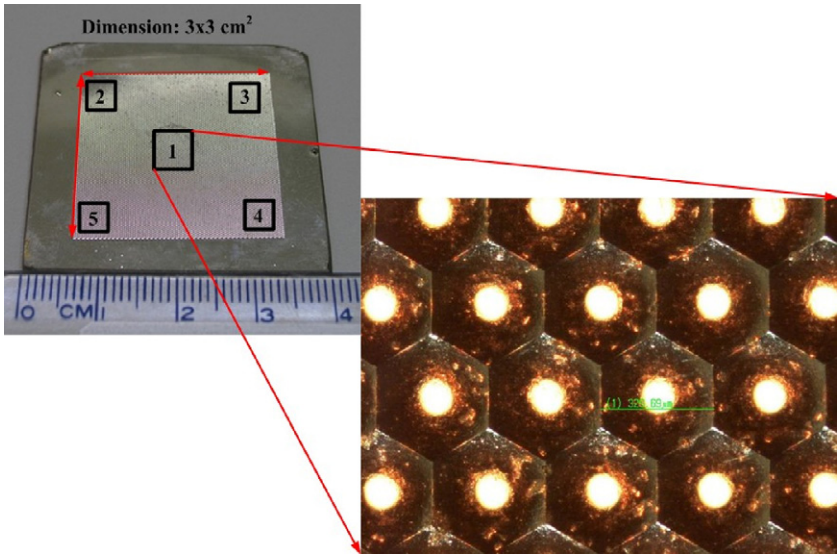

Fig. 4. Ni–Co mold with gapless hexagonal micro-lens array.

Table 1
Variation in average dimension

Point	1	2	3	4	5
Width (μm)	329.69	322.97	330.58	326.58	319.89
Average (μm)			325.94		

forming ability and viscous flow can be enhanced and observed clearly. The dimensions of this micro-lens over the array are measured. Points from 1 to 5 (see Fig. 4) are selected for the measurement. The variation in average dimension is listed in Table 1. It shows that the variation is less than 6.05 μm. Fig. 4 also shows that there is no gap between the micro-lenses, meaning that a gapless micro-lens array has been successfully fabricated using the electroplating process.

Fig. 5 shows the replicated patterns on the BMG material, embossed by the first mold at 150 °C under pressure of 2 MPa. On the other hand, Fig. 6 illustrates the deforming evolution of the replicated patterns onto the BMG material. Excellent replicated patterns can be obtained using a larger pressure level as shown in Fig. 5, with the embossing parameters of 150 °C (423 K) and 2 MPa for 10 s held in the oil hydraulic plates. The glass transition temperature of BMG is about 140 °C (413 K). Therefore, temperature of 150 °C is chosen for the hot embossing experiment. The roughness of the surface quality of the micro-lens shown in Fig. 5 is better than that shown in Fig. 6. It can be explained that a high pressure level enables the viscous flow of the BMG material to fill up the Ni–Co mold completely. As a result, better surface quality and formability are achieved as shown in Fig. 5. The deforming evolution of the micro-lens array on the BMG material with different forming time is shown experimentally in Fig. 6, with parameters of embossing temperature at 150 °C, pressure of 400 kPa and forming time from 1 to 4 min by the spring plates. It

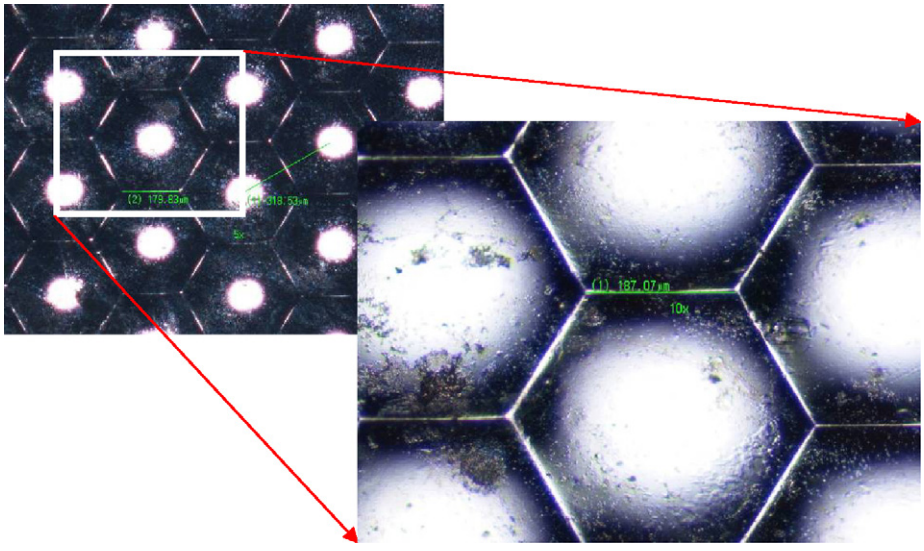

Fig. 5. Replicated patterns on the BMG material imprinted at 150 °C and 2 MPa.

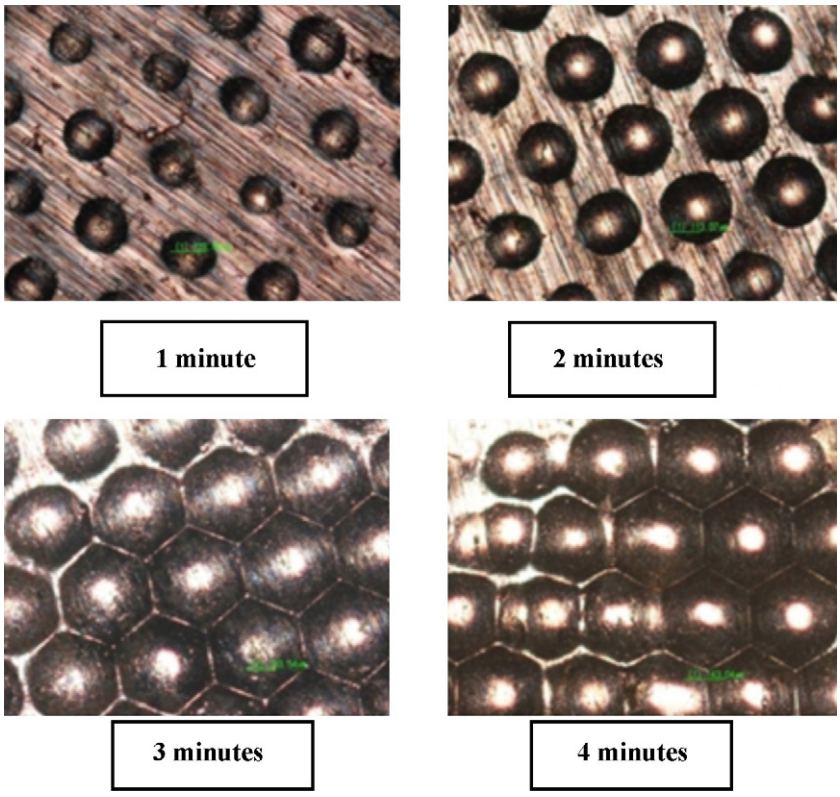

Fig. 6. Deforming evolution of the secondary mold, operated at 150 °C and 400 kPa.

reveals that it takes about 4 min to complete the embossing process.

Fig. 7 shows a similar result. The experimental result shown in Fig. 7 is obtained with different levels of pressures at the same embossing temperature of 150 °C and forming time for 4 min. The result reveals that pressure level of 400 kPa is a better parameter to replicate a micro-lens array compared to others. The result is consistent with that shown in Fig. 2(a), which exhibits a larger strain at a larger pressure level. However, when the embossing time lasts too long, the BMG material may be crystallized. Thus,

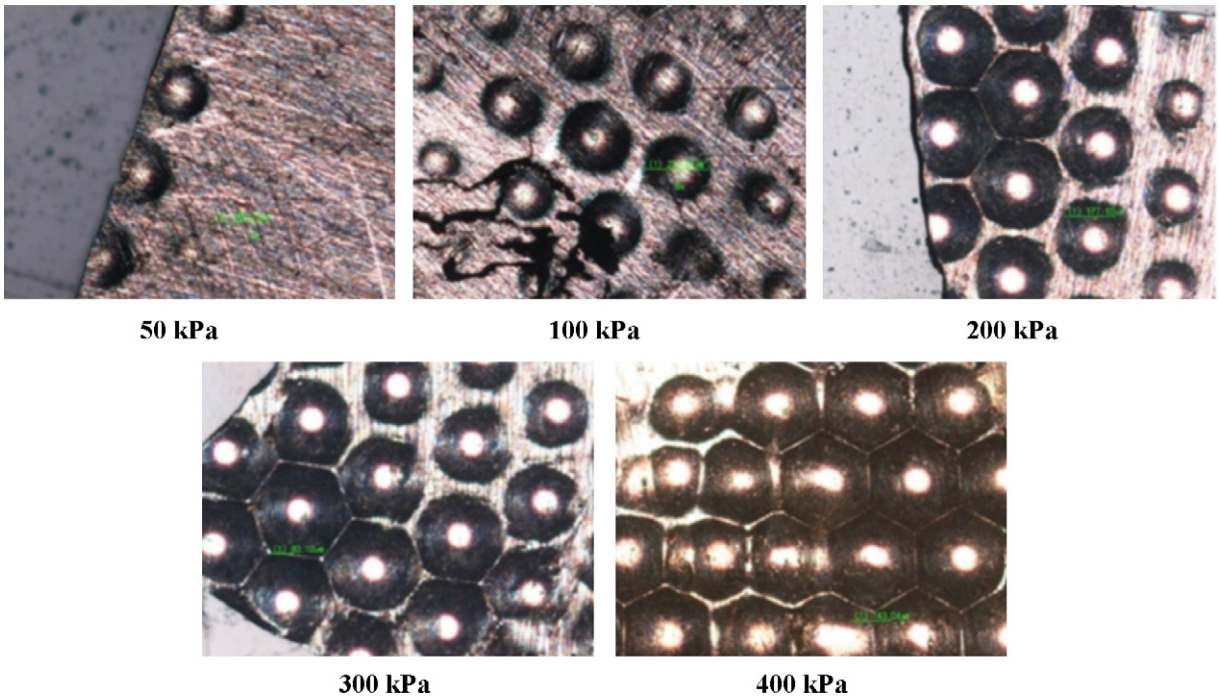

Fig. 7. Experimental results with different pressures at the same forming temperature of 150 °C and the same duration time of 4 min.

the forming time of 4 min is chosen at this experiment. The stress enhanced crystallization phenomena as a function of the stress level, forming time and temperature will be continuously examined in the future study.

Before the embossing process, it can be seen clearly that there are some marks on the surface of a BMG raw material, which is produced during its manufacturing process. To improve this, the surface was polished with abrasive papers of No. 2000. However, parallel bands and marks on the surface are observed clearly in Figs. 6 and 7 after embossing.

Fig. 8(a) is a scanning electron microscopy (SEM) picture of a BMG sample using the oil hydraulic plate system, and Fig. 8

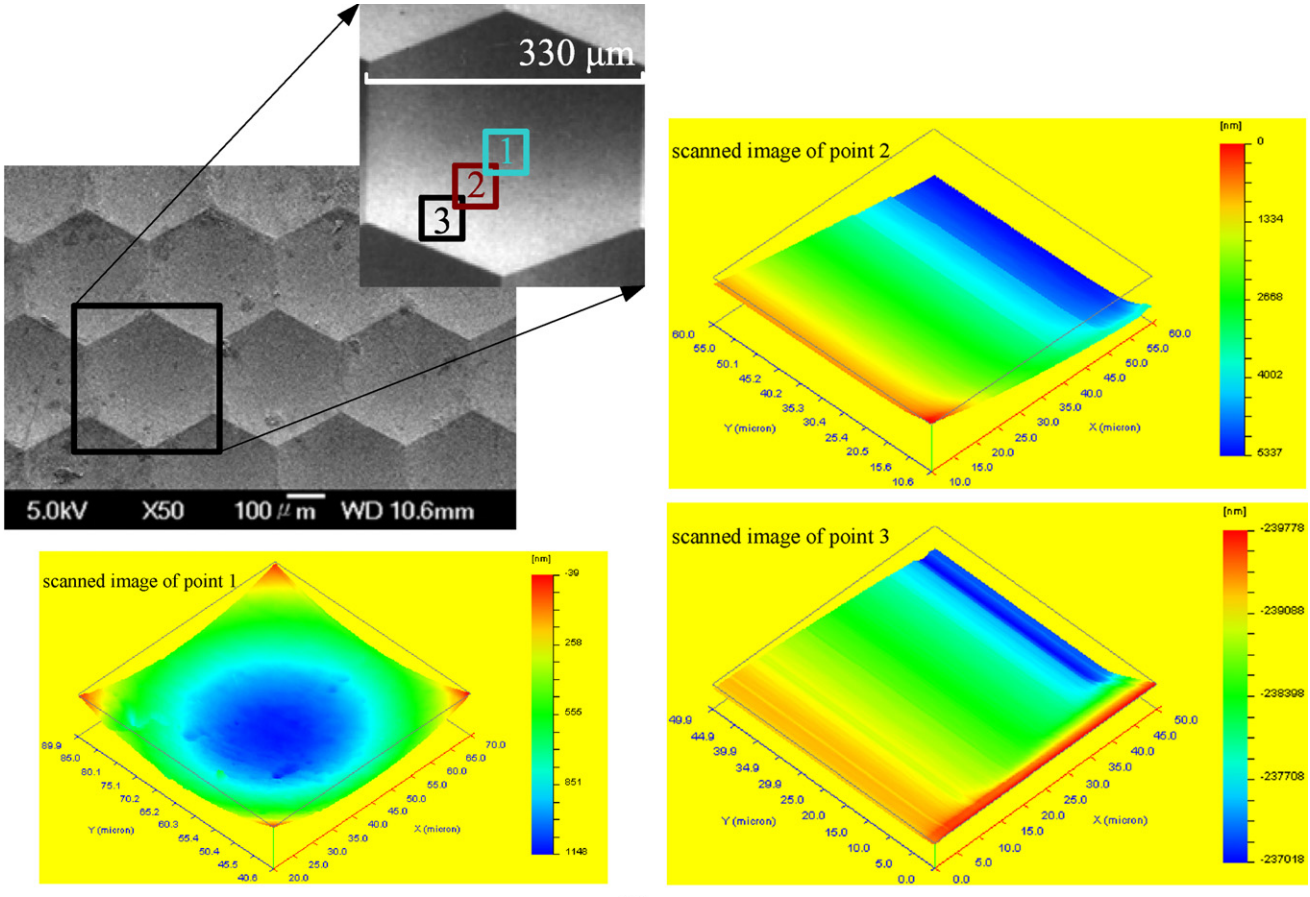

(a)

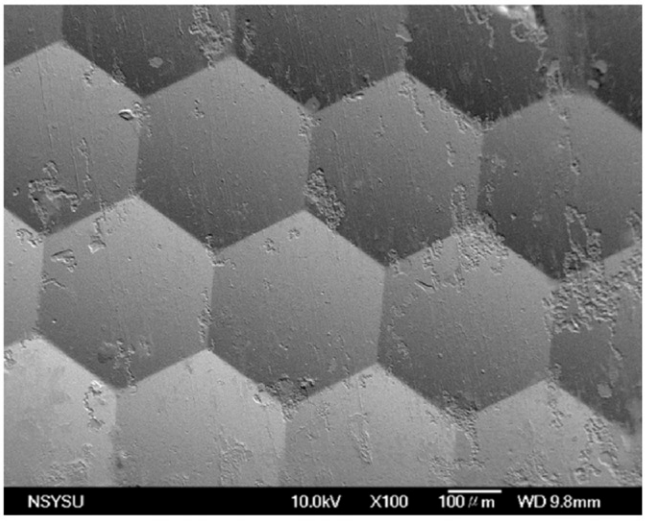

(b)

Fig. 8. SEM micrographs of the BMG samples which are fabricated by (a) the oil hydraulic plate, and the images for the dimension 50 μm × 50 μm of the area 1, 2, and 3 are presented for differences in roughness from the center to the perimeter of a micro-lens by nano indenter system; (b) the spring plate system, at 150 °C and for 4 min. (a) The sample by the oil hydraulic plate system (b) The sample by the spring plate system.

(b) is a SEM photo using the spring plate system. It can be seen in Fig. 8 that there are marks on the surface of a micro-lens. These marks were present on the BMG raw material prior to hot embossing process. Since the BMG raw material is manufactured using metallic mold casting method, the viscous flow of the BMG material causes some marks. Besides, the wear cavity of the Ni–Co mold can transfer some marks to BMG during hot embossing process. It was found that the roughness and the geometry of the sample using the oil hydraulic plate are better than that using the spring plate. The roughness is measured and observed by nano indenter system (From Nano Indenter XP System, MTS co.). By this system, three different points from the center to the perimeter of a micro-lens (see Fig. 8(a)) are scanned. The roughness can be observed roughly in the scanned images. The larger pressure applied in the experiment, the higher the forming degree of the BMG material becomes. Thus, when a higher pressure is applied, a higher transferability can be achieved. The result also indicates that micro-lens using a low pressure level shows more marks left behind than that using a high pressure level. It explains that a larger pressure condition produces a better formability, and more precise and smoother replica can be obtained.

The PMMA sheet with 1 mm in thickness is purchased from Hsintou Company in Taiwan. The T_g of PMMA is around 105 °C. Therefore, the parameters of the hot embossing experiment are set to be 120 °C and 2 MPa. Fig. 9 shows that similar defects on BMG mold are replicated on the surface of the PMMA sheets. The forming pressure of the PMMA is much higher than that of $Mg_{58}Cu_{31}Y_{11}$ material. It means that $Mg_{58}Cu_{31}Y_{11}$ is more deformable material than PMMA. The patterns are replicated completely on the PMMA and they exhibit optical characteristics because clear focused spots are observed. It is noted that the longer the holding time is, the better the surface quality is, as revealed in Fig. 9(b). However, the temperature cannot be too high; neither can the heating time be too long due to the limitation of thermal properties of $Mg_{58}Cu_{31}Y_{11}$. When the holding time is too long, $Mg_{58}Cu_{31}Y_{11}$ may be crystallized to make it become brittle and vulnerable of breaking at high pressure. Therefore, an appropriate forming temperature and holding time are key parameters to the hot embossing process.

Since the maximum scanning dimension by nano indenter system is 100 μm × 100 μm in area, in order to scan the whole profile of 330 μm of a micro-lens, α-step system is used to obtain the images. The profile of micro-lens of Ni–Co mold is convex, the BMG mold is concave, and the final embossed PMMA is convex. The profiles of micro-lens on the Ni–Co mold, the $Mg_{58}Cu_{31}Y_{11}$ mold, and the PMMA are measured and shown in Fig. 10(a), (b), and (c), respectively. For comparison, the three profiles are compared on the same graph as shown in Fig. 10(d). Note that the profile of the concave BMG has been reversed for easy comparison. Comparison of data referring to the first mold, the secondary mold and replicated PMMA are collected in Table 2 where "*H*" is the height, "*W*" is the length of a micro-lens (see Fig. 10(d)). Fig. 10(a) shows the profile of the first mold, which is a convex mold. The convex mold is 745.87 μm in width. Fig. 10(b) shows the profile of the secondary mold, which is a concave mold replicated using the spring plate system. This concave mold is 745.47 μm in width. Fig. 10(c) exhibits the profile of the micro-lens on the PMMA fabricated using the oil hydraulic plate system, which is a convex lens. The convex lens shows 738.66 μm in width. The shrinkage between the first and secondary mold shows 0.05% in shrinkage, whereas the shrinkage between the secondary mold and PMMA replica shows 0.91%.

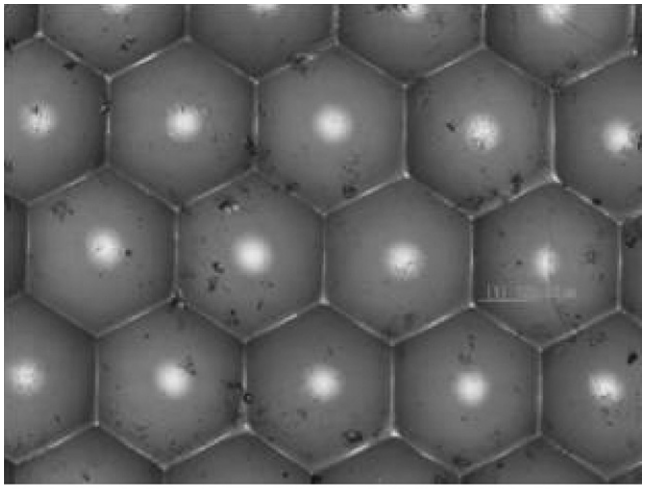

(a)

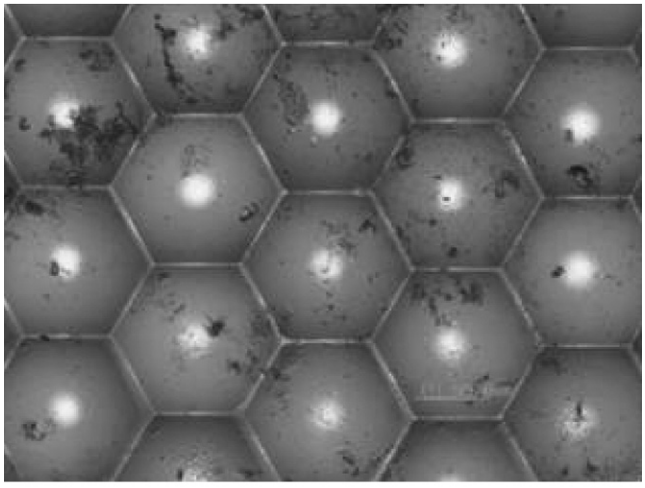

(b)

Fig. 9. Micro-lens array replicated on the PMMA sheets at 120 °C and 2 MPa. (a) 1 min of holding time; (b) 2 min of holding time.

Table 2
Comparison of data referring to 1st mold, 2nd mold and replicated PMMA

	Height (*H*, μm)	Width (*W*, μm)	Shrinkage (%)
Ni–Co mold (1st mould)	~14	~330	0.05
BMG mold (2nd mould)	~13	~330	0.91
PMMA	~13	~330	

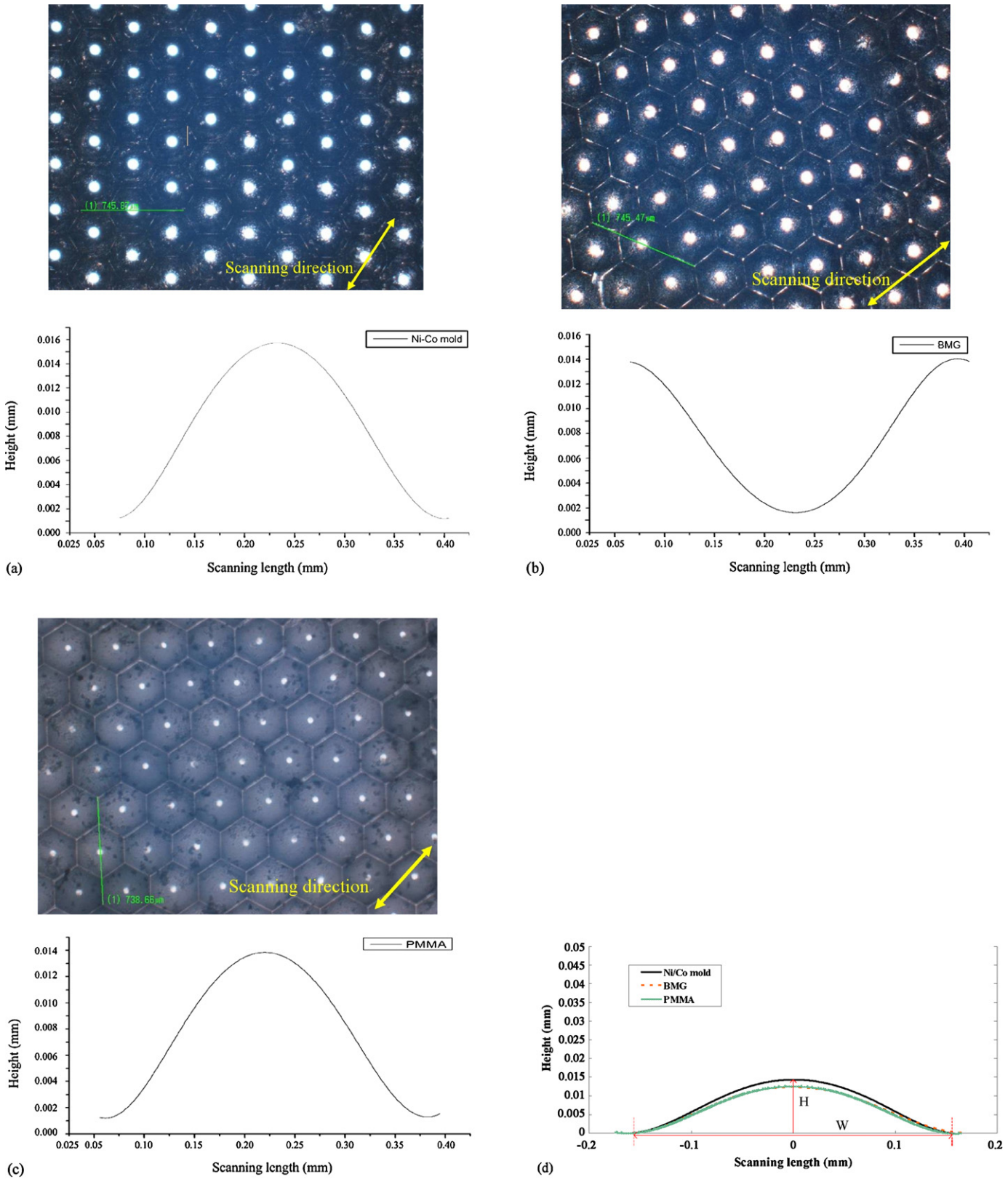

Fig. 10. The profiles of micro-lens on (a) the Ni–Co mold, (b) the $Mg_{58}Cu_{31}Y_{11}$ mold, and (c) the PMMA are measured, respectively; for comparison, (d) the three profiles are compared on the same graph. (a) Micro-lens profile on the Ni–Co mold; (b) micro-lens profile on the $Mg_{58}Cu_{31}Y_{11}$ mold; (c) micro-lens profile on the PMMA; (d) comparison of the surface profiles of the Ni–Co mold, the $Mg_{58}Cu_{31}Y_{11}$ mold, and the PMMA.

5. Conclusion

This study presents a new process to fabricate micro-lens array. The working temperature for embossing is around 423 K. The maximum engineering strains $\Delta L_{max}/L_0$ occurred in the supercooled liquid region reaches 1.52%, 4.07%, 6.63%, 18.72%, and 23.08% under the applied compressive load of 0.8, 2.4, 7.1, 117.8, and 318.5 kPa, respectively. The Ni–Co mold with an inscribed circle 330 μm in diameter has been successfully fabricated using the electroplating process. Excellent replicated patterns can be obtained using a larger applied pressure level. The result reveals that pressure level of 400 kPa and forming time of 4 min are good parameters to replicate a micro-lens array. When high pressure is applied, high transferability of micro-lens can be achieved. The result also indicates that micro-lens using a low pressure level reveals more indented marks left behind than that using a high pressure level. It is noted that the longer the holding time is, the better the surface quality is. The forming pressure of the PMMA is much higher than that of $Mg_{58}Cu_{31}Y_{11}$ material. It means that $Mg_{58}Cu_{31}Y_{11}$ is more deformable material than PMMA. The profiles of micro-lens are examined. The profile of the first mold is 745.87 μm in width. The profile of the secondary mold is 745.47 μm in width. The profile of the micro-lens on the PMMA shows 738.66 μm in width. The shrinkage between the first and secondary mold shows 0.05% in shrinkage, whereas the shrinkage between the secondary mold and PMMA replica shows 0.91%.

Acknowledgements

The authors would like to thank National Science Council for their financial supports to the project (granted number: 95-2221-E-110-093-MY2, 95-2221-E-110-141, and 94-2622-E-110-017-CC3). Also, the authors would like to thank Mr. J.H. Ou for his help in experimental set-up.

References

[1] Y.C. Chang, T.H. Hung, H.M. Chen, J.C. Huang, T.G. Nieh, C.J. Lee, Viscous flow behavior and thermal properties of bulk amorphous $Mg_{58}Cu_{31}Y_{11}$ alloy, Intermetallics 15 (2007) 1303–1308.
[2] O.N. Senkov, J.M. Scott, D.B. Miracle, Composition range and glass forming ability of ternary Ca–Mg–Cu bulk metallic glasses, J. Alloys Compd. 424 (2006) 394–399.
[3] W.Y. Liu, H.F. Zhang, Z.Q. Hua, H. Wang, Formation and mechanical properties of $Mg_{65}Cu_{25}Er_{10}$ and $Mg_{65}Cu_{15}Ag_{10}Er_{10}$ bulk amorphous alloys, J. Alloys Compd. 397 (2005) 202–206.
[4] Z.P. Lu, C.T. Liu, Y. Li, Glass transition and crystallization of Mg–Ni–Nd metallic glasses studied by temperature-modulated DSC, Intermetallics 12 (2004) 869–874.
[5] G. Yuan, T. Zhang, A. Inoue, Structure and mechanical properties of Mg85Cu5Zn5Y5 amorphous alloy containing nanoscale particles, Mater. Lett. 58 (2004) 3012–3016.
[6] G. Yuan, A. Inoue, The effect of Ni substitution on the glass-forming ability and mechanical properties of Mg–Cu–Gd metallic glass alloys, J. Alloys Compd. 387 (2005) 134–138.
[7] R. Busch, E. Bakke, W.L. Johnson, Viscosity of the supercooled liquid and relaxation at the glass transition of the $Zr_{46.75}Ti_{8.25}Cu_{7.5}Ni_{10.0}Be_{27.5}$ bulk metallic glass forming alloy, Acta Mater. 46 (1998) 4725.
[8] P. Pérez, G. Garcés, F. Sommer, P. Adeva, Mechanical properties of amorphous and crystallized Mg–35 wt% Ni, J. Alloys Compd. 396 (2005) 175–181.
[9] P. P_erez, M. Eddahbi, G. Garc_es, F. Sommer, P. Adeva, Mechanical properties of crystallised amorphous Mg–23.5Ni (wt%) alloy, Scripta Mater. 50 (2004) 1039–1043.
[10] Q. Zheng, S. Cheng, J.H. Strader, E. Ma, J. Xu, Critical size and strength of the best bulk metallic glass former in the Mg–Cu–Gd ternary system, Scripta Mater. 56 (2007) 161–164.
[11] U. Wolff, N. Pryds, J.A. Wert, Deformation characteristics of Mg60Cu30Y10 alloy at temperatures near T_g, Scripta Mater. 50 (2004) 1385–1388.
[12] A. Inoue, T. Zhang, T. Masumoto, Glass-forming ability of alloys, J. Non-Cryst. Solids 156–158 (1993) 473.
[13] S. Kagao, Y. Kawamura, Y. Ohno, Electron-beam welding of Zr-based bulk metallic glasses, Mater. Sci. Eng. A 375–377 (2004) 312–316.
[14] T. Shoji, Y. Kawamura, Y. Ohno, Friction welding of bulk metallic glasses to different ones, Mater. Sci. Eng. A 375–377 (2004) 394–398.
[15] Y. Kawamura, Liquid phase and supercooled liquid phase welding of bulk metallic glasses, Mater. Sci. Eng. A 375–377 (2004) 112–119.
[16] Y. Kawamura, T. Shoji, Y. Ohno, Welding technologies of bulk metallic glasses, J. Non-Cryst. Solids 317 (2003) 152–157.
[17] M. Bakkal, A.J. Shih, R.O. Scattergood, Chip formation, cutting forces, and tool wear in turning of Zr-based bulk metallic glass, Int. J. Mach. Tool Manu. 44 (2004) 915–925.
[18] M. Bakkal, A.J. Shih, S.B. McSpadden, R.O. Scattergood, Thrust force, torque, and tool wear in drilling the bulk metallic glass, Int. J. Mach. Tool Manu. 45 (2005) 863–872.
[19] Y. Saotome, K. Itoh, T. Zhang, A. Inoue, Superplastic nanoforming of Pd-based amprphous alloy, Scripta Mater. 44 (2001) 1541–1545.
[20] J.P. Chu, H. Wijaya, C.W. Wu, T.R. Tsai, C.S. Wei, T.G. Nieh, Jeffrey Wadsworth, Nanoimprint of gratings on a bulk metallic glass, Appl. Phys. Lett. 90 (2007) 034101.
[21] M.C. Chou, C.T. Pan, S.C. Shen, M.F. Chen, K.L. Lin, S.T. Wu, A novel method to fabricate gapless hexagonal micro-lens array, Sensor. Actuat. A 118 (2005) 298–306.

Biographies

Dr. C.T. Pan was born in Nauto, Taiwan, Republic of China, in 1969. He received his engineering degree of master and doctor in 1993 and 1998, respectively, from Power Mechanical Engineering Department of National Tsing Hua University in Hsinchu, Taiwan. He was a researcher in the field of laser machining polymer in the TU Berlin (IWF) in Germany from 1997 to 1998 and a researcher of MEMS Division in the MIRL/ITRI, Hsinchu in Taiwan from 1998 to 2003. He joined National Sun Yat-Sen University, Kaohsiung, Taiwan, Republic of China, as an assistant professor in 2003. His current research interests focus on MEMS, NEMS, and LIGA process.

Mr. T.T. Wu was born in Yunlin, Taiwan, Republic of China, in 1981. He received his engineering degree of master in 2005 from Mechanical and Electro-Mechanical Engineering Department of National Sun Yat-Sen University in Kaohsiung, Taiwan. He is now a candidate for doctor's degree in the Mechanical and Electro-Mechanical Engineering research institute of Sun Yat-Sen University, Kaohsiung, Taiwan, Republic of China. His current research interests focus on NEMS, MEMS, and LIGA process.

M.F. Chen was born in Tainan, Taiwan, Republic of China, in 1980. He received his engineering degree of bachelor in 2003, respectively, from Mechanical Engineering Department of National Sun Yat-Sen University in kaohsiung, Taiwan. He is studying in the Mechanical Engineering research institute of Sun Yat-Sen University, Kaohsiung, Taiwan, Republic of China. His current research interests focus on MEMS, NEMS, and LIGA process.

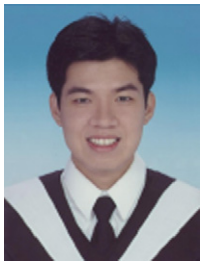

Mr. Y.C. Chang was born in Kaohsiung, Taiwan, Republic of China, in 1978. He received his master degree in 2003, from Feng Chia University. He is a PhD candidate in National Sun Yat-Sen University. His current research interests include the conductive polymer, fibre material, bulk metallic glass, viscous flow behavior of metallic glass, and micro-forming of metallic glass.

Dr. C.J. Lee was born in Kaohsiung, Taiwan, Republic of China, in 1979. He received his PhD degree in 2006, from National Sun Yat-Sen University. He is a post-doc researcher in National Sun Yat-Sen University. His current research interests include the friction stir processing, nano materials and composites, and micro-pillar amorphous alloy mechanical properties.

Dr. J.C. Huang was born in Kaohsiung, Taiwan, Republic of China, in 1957. He received his PhD degree in 1986, from University of California, Los Angles, USA. He was a post-doc researcher in UCLA and Los Alamos National Laboratory from 1986–1989. He joined National Sun Yat-Sen University as an associate professor in 1989, and advanced to full professor in 1994 and chair professor in 2006. His current research interests include the metallic glasses, nano materials and composites, and transmission electron microscopy.